Enhanced osteoblastic activity and bone regeneration using surface-modified porous bioactive glass scaffolds

San Miguel, B ; Kriauciunas, R ; Tosatti, S ; Ehrbar, M ; Ghayor, C ; Textor, M ; Weber, Franz E

Abstract: The potential use as a bone substitute material of a three-dimensional bioactive glass fiber scaffold composed of Na(2)O-K(2)O-MgO-CaO-B(2)O(3)-P(2)O(5)-SiO(2) (BG1) was investigated in this work. Scaffolds were pre-treated with simulated body fluid (SBF) to promote the formation of two different bone-like apatite layers on their surfaces. The topography and roughness of the deposited layers were assessed by scanning electron microscopy (SEM), while the chemical composition and structure using X-ray photoelectron spectroscopy (XPS) and Raman spectroscopy, respectively. Based on surface analysis, the bioactive glass surfaces were ranked from smoothest to roughest: 0 SBF (untreated), 1x SBF and 2x SBF. A calcium-deficient carbonated hydroxyapatite (HCA) layer was present on both SBF-treated scaffolds, with higher number and larger bone-like apatite nodule formation in the 2x SBF case. MC3T3-E1 preosteoblasts showed a more flattened morphology and higher cell proliferation on the nontreated scaffolds; whereas, cells were more elongated and had higher osteoblastic activity on SBF-treated samples. In vivo results in a rabbit calvarial bone defect model showed enhanced bone formation with SBF pretreated scaffolds, compared with untreated ones, commercially available Perioglass particles and empty defects. Our findings demonstrate that the formation of a rough HCA layer on bioactive glass porous scaffolds enhanced preosteoblast maturation in vitro, as well as bone formation in vivo.

DOI: https://doi.org/10.1002/jbm.a.32773

Enhanced osteoblastic activity and bone regeneration using surface-modified porous bioactive glass scaffolds

Blanca San Miguel,[1] Rytis Kriauciunas,[1], Samuele Tosatti,[2] Martin Ehrbar,[1] Chafik Ghayor,[1] Marcus Textor,[2] Franz E. Weber[1*]

[1] University Hospital Zurich, Dept. of Cranio-Maxillofacial Surgery, Oral Biotechnology & Bioengineering, Frauenklinikstrasse 24, 8091 Zurich, Switzerland.

[2] Laboratory for Surface Science and Technology, Department of Materials, ETH Zurich, Wolfgang-Pauli-Strasse 10, 8093 Zurich, Switzerland.

***Correspondence to:** Franz E. Weber; email: franz.weber@zzmk.uzh.ch, Tel: +41 44 255 5055, Fax: +41 44 255 4179

Abstract: The potential use as a bone substitute material of a three-dimensional bioactive glass fibre scaffold composed of $Na_2O–K_2O–MgO–CaO–B_2O_3–P_2O_5–SiO_2$ (BG1) was investigated in this work. Scaffolds were pre-treated with simulated body fluid (SBF) to promote the formation of two different bone-like apatite layers on their surfaces. The topography and roughness of the deposited layers were assessed by scanning electron microscopy (SEM), while the chemical composition and structure using X-ray photoelectron spectroscopy (XPS) and Raman spectroscopy, respectively. Based on surface analysis, the bioactive glass surfaces were ranked from smoothest to roughest: 0 SBF (untreated), 1x SBF and 2x SBF. A calcium-deficient carbonated hydroxyapatite (HCA) layer was present on both SBF treated scaffolds, with higher number and larger bone-like apatite nodule formation in the 2x SBF case. MC3T3-E1 preosteoblasts showed a more flattened morphology and higher cell proliferation on the non treated scaffolds, whereas cells were more elongated and had higher osteoblastic activity on SBF-treated samples. *In vivo* results in a rabbit calvarial bone defect model showed enhanced bone formation with SBF pre-treated scaffolds, compared to untreated ones, commercially available Perioglass® particles and empty defects. Our findings demonstrate that the formation of a rough HCA layer on bioactive glass porous scaffolds enhanced preosteoblast maturation *in vitro*, as well as bone formation *in vivo*.

Keywords: Bioactive glass, Bone regeneration, Osteoblast, Scaffold, SBF

INTRODUCTION

More than one million patients are treated every year to manage bone defects of congenital origin, generated after tumor resection and fractures, as well as to perform spine fusions, and to restore osseous sites in joint and dental implantology.[1] The standard approaches currently use bone autografts. They have inherent limitations, including availability of graft material and non-optimal shape, requirement of secondary surgery to access autograft material, extended patient recovery time and site morbidity.[2] Allogenic bone or xenogenic grafts have been considered as an alternative. However, they still pose the risk of disease transmission, loss of biological and mechanical properties following explantation, and high costs, which altogether limit their use.[3]

An ideal scaffold for bone regeneration is biocompatible and provides a three-dimensional network for cells and bone to grow within it, namely by the creation of an interconnected macroporous structure with pore diameter of at least 100 μm. Furthermore, it should promote cell adhesion and activity, ideally towards the osteoblastic phenotype, resorb along with new bone formation, and its mechanical properties should match those at the implantation site.[3] In efforts to develop alternative materials for bone autografts, synthetic bone substitute scaffolds constitute promising candidates. In this respect, many materials are being currently studied including natural and synthetic polymers, inorganic materials and composites. In the field of inorganic biomaterials, besides ceramics and calcium phosphates (i.e. hydroxyapatite (HAP), tricalcium phosphate), bioactive glasses appear to be promising bone substitutes.[4] They are able to promote osteoconduction, since they allow for direct bone bonding and in-growth, as well as sufficient vascularization. Moreover, they are bioresorbable and have potential osteoproductive properties, which provide a good environment for bone cells to grow and differentiate.[5]

By definition, the “bioactivity” associated with bioactive glass materials relates to their ability to elicit a specific biological response at the interface of the material, which

results in the formation of a direct bond to the tissues surrounding it.[6] This process starts when bioactive glasses are immersed into biological fluids *in vivo* or simulated body fluid (SBF), cell culture medium or other buffered electrolyte solutions *in vitro*. In these cases, a series of events occur via ion leaching and exchange with the surrounding solution, which lead to calcium phosphate precipitation and final bone-like apatite layer formation onto the bioactive glass surface.[7,8] This ionic dissolution, together with the slight alkalinization thereby induced,[9] have been associated with the osteoproductive properties of bioactive glasses.

Most of the bioactive glasses studied so far have a particulate shape (i.e. Novabone®, Perioglass®), or are produced in form of block material, which is difficult to shape and has a very low surface area to volume ratio (SA/V). The particulate material can easily adapt to any required shape, has a high SA/V ratio and therefore improved osteoconductive properties due to enhanced ionic product dissolution and surface reactivity.[10,11] One of the major disadvantages of this particulate form of bioactive glasses are their difficult placement and maintenance within the defect, together with poor mechanical properties and low interconnectivity.[12] Until the 90s, it was difficult to manufacture these glasses in other shapes rather than the above mentioned, due to the required thermal processing of the compositions available. Two approaches were considered to circumvent this flaw: one includes the use of sol-gel bioactive glasses that can be manufactured as porous blocks, and the other one comprises melt-derived materials with "large working range compositions",[13] such as the "BG1" investigated in this work. These compositions have improved processing properties which allow them to be manufactured as fibres of different dimensions. After sintering, those fibres can form three-dimensional, easy to handle porous scaffolds, with macroporous structure, interconnected porosity, and mechanical properties more similar to those of human cancellous bone.[12,14]

In the work presented here, the capacity of BG1 scaffolds to be used as bone substitute materials was evaluated. Initially, an *in vitro* analysis of their bioactivity after pre-treatment under two different SBF conditions to promote the formation of a bone-like apatite layer on their surface was performed, and the resulting deposited layers were characterized. Subsequently, preosteoblast initial cell attachment and morphology, as well as osteoblastic response *in vitro* were assessed, followed by an *in vivo* study to test their bone regeneration

MATERIALS AND METHODS

BG1 scaffold manufacturing process

BG1 glass fibres with an average diameter of 75 μm were produced by melt spinning, with the following nominal composition "BG1" (% wt): 53.6% SiO_2, 13.2% CaO, 11.9% Na_2O, 15.1% K_2O, 3.2% MgO, 2.0% P_2O_5 and 1.0% B_2O_3. These fibres were further cut to a length of 3 mm and poured into a commercial grade II titanium mould of 8 mm in diameter and 10 mm height at Inion OY (Tampere, Finland). This mould containing the fibres was placed into a furnace to undergo a sintering process for 25 minutes at 630°C, rendering a relative porosity of 70% and mean pore size of 300-400 μm, as previously described.[14]

SBF preparation and pre-treatment

SBF was prepared by mixing the following reagents at room temperature under stirring conditions, and adjusting the pH to a final range of 7.30-7.35: NaCl, Na_2SO_4, $NaHCO_3$, KCl, $K_2HPO_4.3H_2O$, $MgCl_2.6H_2O$, $CaCl_2$, $C_4H_{11}NO_3$, HCl (5N) (Sigma-Aldrich, Buchs, Switzerland). Prior to use in cell culture assays, SBF solutions were filtered sterile through a 0.22 μm sieve (Millipore, Zug, Switzerland). The final molarity of the 1x SBF solutions, similar to the ionic blood plasma composition,[8] is shown in Table I.

After sterilizing the scaffolds by dry heat at 180°C for 2 hours, the so called "1x SBF" and "2x SBF" scaffolds were subjected to a static four day incubation at 37°C in 1x SBF, and

eight days in double concentrated SBF respectively, with media change after the first four days. The surface area to volume ratio was maintained at 0.5 cm^{-1} in both cases. Surface area (SA) was calculated individually for each scaffold using the following formula:

$$SA\ (cm^2) = \frac{2.\ w}{\rho.\ \frac{1}{2}.\ (\phi)} \qquad (1)$$

Where w = scaffold's weight (g), ρ = glass density = 2.52 g/cm^3, and ϕ = fibre diameter = 0.0075 cm. After the corresponding SBF incubation period at 37°C, each scaffold was rinsed with sterile distilled H_2O to stop any on-going reaction, washed with 70% EtOH, and thereafter dried overnight at 37°C. Non-treated scaffolds were used as controls.

Scaffold characterization

Raman spectra were measured in a Renishaw 2000 micro-spectrometer equipped with a He/Ne laser of 632.8 nm wavelength, at EMPA, Dubendorf, Swirzerland. A Leica 50 x/0.75 objective was used to focus the laser beam and to obtain the Raman signal. The spectra of three different spots from each sample (n=6) were recorded three times during 30 seconds and finally averaged. X-ray photoelectron spectroscopy (XPS) spectra were recorded with a SIGMA 2 system (ThermoFischer, England) using non-monochromatized AlKα radiation at 300 W (15 kV). For each sample, 0-1100 eV survey spectra were recorded with an electron-energy analyzer pass energy of 50 eV, and narrow scans at pass energy of 25 eV. The spectra were corrected for sample charging (eV shift), with the adventitious C1s peak at binding energy of 285.0 eV used as an internal reference. The XPS data were quantified by using peak areas (measured after Shirley background substraction) and Scofield sensitivity factors (R.S.F).[15]

Scanning electron microscopy

Bioactive glass scaffolds were subjected to scanning electron microscopy (SEM) at EMZ, University of Zurich, Switzerland. Briefly, at the indicated time points, scaffolds were washed in PBS at 37°C (Invitrogen, Basel, Switzerland), and immediately fixed in 3% glutaraldehyde solution for 30 min. Cellular lipids were post-fixed in 2% osmium tetraoxide for 15 minutes at room temperature, cells were dehydrated through increasing concentrations of ethanol (50-70-95-100%), and finally twice with absolute ethanol. Thereafter samples were critical point dried, sputter coated with 10 nm platinum and viewed using a field emission scanning electron microscope (Zeiss Supra 50V) operated at 5 kV. Images were obtained with the In-Lens detector.

Cell culture on BG1 scaffolds

Scaffolds were pre-incubated for 1 hour in MEM-alpha with 10% (v/v) FBS, and 100 U/ml penicillin - 100 µg/ml streptomycin (Invitrogen, Basel, Switzerland). Upon media aspiration, MC3T3-E1 cells were seeded as a micropellet (10 µl of cell suspension) to obtain 5000 cells/cm^2 on each scaffold. After 1h 30 min, culture media was added to each scaffold-containing well. 24 h after seeding, media was exchanged and supplemented with 50 µg/ml ascorbic acid (Sigma-Aldrich, Buchs, Switzerland), and thereafter replaced twice a week. MC3T3-E1 cells were chosen in this study due to their high levels of osteoblastic differentiation, mineralised extracellular matrix deposition, and a similar behaviour to primary osteoblasts, which altogether makes them a widely used model for in vitro bone formation. [16]

Alkaline Phosphatase (ALP) activity and total protein measurement

Scaffolds seeded with cells were rinsed in PBS after one week in culture, and placed into 1.5 ml polypropylene tubes, where they were crushed with a stainless steel pellet pestle. Subsequently, cells were lysed in 56 mM of 2-amino-2-methyl-propan-1-ol, 1 N HCl,

0.2% Triton X-100 (Sigma-Aldrich, Buchs, Switzerland), at pH 10. The debris of the scaffold were removed by short centrifugation, and ALP activity was determined by incubation of the cell lysate in 20 mM of *p*-nitrophenylphosphate (Fluka Chemicals, Buchs, Switzerland), containing 4 mM of $MgCl_2$, at 37°C for 10 minutes. The reaction was stopped by the addition of NaOH 1N. The enzymatic activity was determined by the rate of hydrolysis of *p*-nitrophenyl phosphate, which was measured at a wavelength of 405 nm and normalized to total protein content by the Bradford assay, using an albumin standard.[16] The absorbance of the solution was measured using a spectrophotometer (Spectronic Genesys™ 2PC, Spectronics Instruments, NY, USA), at a wavelength of 570 nm.

DNA quantification

In parallel with ALP activity determination, an aliquot of each cell lysate was diluted 1:10 in Tris buffer 100 mM (Tris Ultrapure Base, ICN Biomedicals, GBMH, Germany), pH=6.5, 1 mM EDTA. Samples were then vortexed and thereafter centrifuged at 13000 rpm for 15 min at 4°C. DNA standard (Lambda DNA, Invitrogen, Basel, Switzerland) dilutions were prepared in ALP lysis buffer (0.2% Triton X-100 in 56 mM of 2-amino-2-methyl-propan-1-ol, 1 N HCl (Sigma-Aldrich, Buchs, Switzerland) at pH 10, and further diluted 1:10 in Tris buffer. Picogreen (Invitrogen, Basel, Switzerland) was applied in equal volume to each sample and standard DNA vial, followed by vortexing, according to the supplier's instructions. Cell samples and standard DNA fluorescence were measured at 480 nm excitation and 520 nm emission in a BMG FLUOStar Optima (BMG Labtech GmbH)**.**

Alizarin-Red calcium nodule formation assay

Cell matrix calcium deposition was analyzed after two weeks in culture by staining the samples with Alizarin Red dye (AR-S, Sigma-Aldrich, Buchs, Switzerland). Briefly, scaffolds were washed once with PBS (pH 7.4), fixed during 1 h at room temperature in 70% EtOH,

followed by staining with 40 mM Alizarin red in H_2O, pH 4.2, during 10 minutes, while shaking.[16] After staining, cultures were washed five times with H_2O, followed by a 15 minutes wash in PBS. The stained matrix was imaged for qualitative analysis at 400 dpi, using a flat bed scanner (Epson 1640SU), and thereafter incubated in 10% hexadecylpyridinium chloride (Sigma-Aldrich, Buchs, Switzerland), in 10 mM sodium phosphate, at pH 7.0 during 1h to solubilize calcium-bound AR-S. The absorbance of the resulting solutions was measured at 562 nm (Spectronic Genesys™ 2PC, Spectronics Instruments, NY, USA).

pH measurement

The pH of the MC3T3-E1 seeded scaffold's supernatant was measured in parallel with tissue culture polystyrene (TCPS) cell culture supernatant, grown in a humidified incubator at 37°C with 5% CO_2 and 95% air, using an Orion 420A+ Thermo electron corporation electrode. pH was recorded for up to 7 days. At each time point, an aliquot of each supernatant was withdrawn, combined in triplicate with samples under the same conditions, and pH values were measured thereafter.

***In vivo* study**

All surgeries were performed under a protocol approved by local authorities (Veterinary Office, Zurich). Four full thickness bone defects were created in a rabbit calvarial model with a 6 mm trephine, two in the parietal and another two in the frontal sites (non-critical size defects). The dura matter was kept intact with minimal invasion during surgery, while the periosteum was removed. The surgeries were performed after sedating the animals with Ketamine under general anaesthesia by a Halothan-N_20 inhalation method. Empty defects were compared to those treated with commercially available Perioglass®, defects filled with an earlier version of porous Bioglass scaffolds of 80% porosity, or the

corresponding 1x SBF treated scaffolds. After placement of the materials, the soft tissues were closed with sutures, and analgesia was delivered by an injection of Novalgin (50 mg/kg). After 4 weeks, four rabbits were sacrificed following sedation with barbiturates via an overdose of Ketamine, upon which the calvarial bone was excised. Subsequently, an X-ray image was taken from the calvarial area of each specimen to locate the middle section of the created defects. Thereafter, samples were dehydrated in graded ethanol series, namely 48 h in 40% ethanol, 72 h in 70% changed every 24 h, 72 h in 96% and a final 72 h in 100% ethanol. Samples were placed in xylene for 72 h to solubilize the fat, infiltrated in methyl methacrylate (MMA) (Fluka Chemicals, Buchs, Switzerland) for 72 h, followed by three days in 100 ml MMA + 2 g dibenzoylperoxid at 4°C (Fluka Chemicals, Buchs, Switzerland). Afterwards, they were embedded in 100 ml MMA + 3 g di-benzoylperoxid + 10 ml Plastoid N or dibutylphtalate, and allowed to polymerize at 37°C in an air tight water bath. Histological sections were prepared from the middle of the defects and stained with Goldner Trichrome. Samples were thereafter analyzed via quantitative analysis of different tissue components by applying standard morphometrical techniques using a Zeiss integration plate eye piece grid.[17] Bone tissue counts (dark green) were measured directly under the light microscope at a magnification of 160 x, using a superimposed eyepiece test grid of 50 points and 25 cycloid lines.

Statistical analysis

SPSS 12.0.1 software was used to calculate mean values and standard deviation of the raw data. For statistical analysis, Student's 2-tailed t-test was applied after initial ANOVA test. ANOVA test was performed by using Excel software, and t-test for statistical significance by means of SPSS 12.0.1 software. Statistical significance was accepted for $P < 0.05$, unless otherwise indicated.

RESULTS AND DISCUSSION

Characterization of the surface layer deposition on SBF-treated scaffolds

In order to promote the bioactivity (bone bonding capacity) of the BG1 bioactive glass scaffolds, they were pre-treated with simulated body fluid solution (SBF) to induce the formation of a surface apatite-like layer[8]. SEM analysis was carried out to observe the features of the deposited layer after each SBF treatment, as well as the scaffold's surface characteristics prior to treatment. SBF pre-treated scaffolds showed an apatite-like rough layer deposited on their fibre surfaces (1x SBF and 2x SBF), whereas non-treated scaffolds (0 SBF) revealed a smooth surface (Fig. 1.a). After 1x SBF treatment, sparse hemispherical nodules of up to 5 μm in diameter precipitated randomly on the scaffold's surface, at a density of 5000 ± 1275 per mm^2 (Fig. 1.b.1). 2x SBF treated scaffolds showed a significantly higher density of spherical nodule formation (8500 ± 2010) per mm^2, accompanied by a secondary globular structure with hemispherical morphology and diameters in the range of 10-20 μm (Fig. 1.b.4). These globular structures were either independent or associated with the smaller spherical features (Fig. 1.b.5). In addition, some nodules aggregated forming clusters, which frequency of appearance was also higher after 2x SBF treatment (Fig. 2). At the nanometer scale, as seen at higher magnifications in Figure 1.b.3,6, both 1x SBF and 2x SBF treatments produced apatite-like layers with the same surface morphology, where sub-micron needle-like crystals typical of microcrystalline apatite were present. These SEM images confirmed the deposition of a rough layer onto the scaffold's surface, with different nodule formations. These nodules were most abundant in the higher concentrated and longer exposure of the 2x SBF treatment (Fig. 2), correlating with higher ionic concentrations in solution, which are known to facilitate calcium-phosphate nucleation and growth of apatite crystals.[2,18]

Raman vibrational modes and degree of surface crystallinity

Raman spectroscopy analysis was carried out to determine the nature of the surface layer deposited onto the scaffolds. The Raman modes of the apatite-like layer grown on the bioactive glass surface after immersion in SBF were similar to those of the natural bone mineral phase of carbonated hydroxyapatite (HCA). Characteristic peaks included the PO_4^{3-} ν_1 stretching mode at 964 cm^{-1} (symmetric stretching vibration of P-O from PO_4^{3-} tetrahedral in HAP crystals), which was slightly shifted to 960 cm^{-1} (Fig. 3). This shift suggested the existence of type B carbonated hydroxyapatite, similar to that found in biological bone.[19] The ν_2 phosphate domain included two bands at 432 cm^{-1} and 450 cm^{-1}, the latter mainly observed in the 2x SBF treated samples. The PO_4^{3-} ν_3 mixed phosphate vibration around 1070 cm^{-1}, which also corresponds to the ν_1 stretching mode of carbonate ions, included the contribution of both anionic groups. Finally, the phosphate ν_4 mode exhibited two main peaks at 589-597 cm^{-1} and 612 cm^{-1} respectively. These values were slightly shifted with respect to pure hydroxyapatite, which again could be due to modifications of the phosphate environment induced by carbonate substitution in type B carbonated hydroxyapatite. The spectra of the non-treated 0 SBF materials showed the expected silica glass main stretching modes, and no presence of calcium phosphate.[20]

It has been described that a thin layer of amorphous carbonated apatite (ACP) is formed after 24h of bioactive glass immersion in SBF (1x SBF). This layer grows thicker with time in solution, turning into calcium deficient crystalline hydroxyapatite after 4 days, which is similar to the bone mineral phase.[21] Typical vibrational modes of carbonated hydroxyapatite were observed after both SBF treatments performed, although pre-incubation in 2x SBF seemed to deposit a thicker HCA layer, as indicated by the more intense peak at 690 cm^{-1}. This peak has been shown to increase with immersion time and to correlate with thicker layer deposition.[22]

Surface XPS elemental composition analysis

The survey spectra of the three surfaces analyzed are shown in Fig. 4, while the elemental composition of Ca 2p, P 2p, O 1s, Na 1s, Si 2p, K 2p and C 1s is given in Table II. Prior to SBF treatment, the main detected elements of the scaffolds surface, apart from adventitious C, were silicon, followed by K, Na and Ca, with atomic percentage values correlating with the initial glass composition. After treatment with SBF, Si surface concentration decreased sequentially for the 1x SBF samples, and more so for the 2 x SBF treatments, while Ca and P concentration increased in both cases, reaching similar levels. Na and K were no longer detectable, indicating that the substrate surface became coated with a calcium phosphate layer thicker than the information depth of XPS. Hydroxyapatite theoretical Ca, P and O elemental composition is shown as a reference included in Table II.[23] The calcium phosphate formed on SBF-treated surfaces also contained carbonate groups as previously indicated by Raman analysis, and its chemical composition was similar to biological calcium phosphates.[24] In our samples, C 1s content in BG1 bioactive glass SBF treated scaffolds is expected to originate from both adventitious (hydrocarbon), and carbonate formation, whereas oxygen originates mainly from the phosphates and carbonates precipitated in association with Ca. Calcium deficiency as experimentally observed from Ca/P ratios of 1.30 compared to theoretical 1.67 of crystalline hydroxyapatite for both SBF treatments,[23] could be explained by a higher carbonate content as Raman analysis already suggested. After 1x SBF and 2x SBF treatments, the HCA-formed layer composition was very similar, except for lower Si content and slightly higher Ca, P and C concentration for 2x SBF-treated scaffolds, suggesting the presence of a thicker HCA layer.[25] The only differences between the 1x SBF and 2x SBF treatments seems to be the rougher and thicker rougher layer (at the microscale level) formed after the 2x SBF treatment, whereas their chemical composition as well as HCA structures were very similar.

Cell adhesion and morphology on the different scaffold HCA surfaces

MC3T3-E1 pre-osteoblasts seeded onto the smooth surface of non-treated scaffolds (0 SBF), exhibited a rounded and flattened morphology with smooth cell extensions in contact with the surface (Fig. 5, 0 SBF). Alternatively, more elongated/spindle-shaped and thicker cells were present on the rougher surfaces (1x SBF and 2x SBF), with irregular processes that extended across the precipitated nodules and globular structures, especially in the 2x SBF case (Fig. 5.7,8).[26,27] Cells seeded both on the 1x SBF and 2x SBF pre-treated scaffolds projected filopodia, creating individual contacts with the surface and anchoring points for cell adhesion. Some authors have suggested that the existence and creation of more cellular filopodia creates areas to which a bigger surface area of the cell can adhere and this, in turn, may promote faster and higher amount of mineral-like nodule formation in the longer term.[28]

After one week in culture, cells spanned the gaps among fibers, producing their own extracellular matrix and allowing for further cell adhesion and proliferation. Details of cells seeded onto 1x SBF and 2x SBF scaffolds are shown at different degrees of magnification in Figure 6. Note the dense extracellular matrix (ECM) layer formed with full scaffold coverage in Fig. 6.a,2 and Fig. 6.a.4, as well as the close association of cells with BG1 fibers through cell filopodia sprouting out of the cell membrane (Fig. 6.a.3). In addition, in Figure 6.b.1, a detail of cell anchorage onto precipitated apatite-like nodules is shown, depicting the tight junction and active processes occurring at these points. In Figure 6.b.2, an example of a 2x SBF-treated scaffold completely covered by cells and ECM after one month is shown. Collagen fibers can be seen associated with cells and ECM covering previously formed carbonated hydroxyapatite nodules, in addition to newly formed ones being deposited onto the ECM (Fig. 6.b.2, arrows).

Osteoblast activity on the different BG1 scaffolds

In order to determine whether the maturation of MC3T3-E1 pre-osteoblastic cells was affected by the presence of the carbonated hydroxyapatite layer and its surface features, osteoblast early (ALP activity) and late maturation assays (calcium deposition), were performed. After one week in culture, ALP activity of cells seeded onto pre-coated scaffolds increased twofold when compared to untreated controls (0 SBF), although no difference was observed between the two SBF treatments (Fig. 7.a). 2x SBF scaffold pre-treatment caused a 50% increase in calcium nodule deposition after 2 weeks, although results were not significantly different to 1x SBF scaffolds or untreated ones (Fig. 7.b). Total protein content was higher for both SBF-treated scaffolds with induced HCA layer formation, suggesting more ECM production per cell (Fig. 7.c). Alternatively, DNA content was higher for the non-treated scaffolds, indicating higher cellular proliferation in these cases (Fig. 7.d). It might be hypothesized that preosteoblastic cells were more sensitive to changes from bioactive glass smooth surface to the presence of a rough HCA layer, than to further differences observed once this layer was present. These results are in agreement with other studies where rough surfaces have been shown to promote osteoblastic maturation and protein production, while suppressing their growth.[29,30]

pH-values of BG1 scaffolds cell culture supernatant

In parallel with cell activity analysis, cell culture supernatant pH values were measured to detect possible media alkalinization, since bioactive glass materials are known to cause this effect due to their ionic products.[9] The pH of all scaffold-containing samples was significantly higher than control media (cells grown on TCPS) at all the time points analyzed ($P<0.01$) (Fig. 8). Moreover, both SBF treatments yielded higher pH than non pre-immersed scaffolds after one and four days in culture ($P<0.05$), although no differences were observed

by day 7. Small pH changes of 0.05-0.2 units, have been shown to promote osteoblastic activity.[31,32] In addition, the ionic dissolutions products of bioactive glass have been claimed to have osteoproductive properties.[33] In this study, even though the ionic dissolution composition was not assessed, the pH values of SBF-treated scaffolds' culture media was higher during the first days in culture. This initial higher pH suggests an increased cationic content, which levelled off after one week, in the same way as other studies have shown.[18] The fact that both SBF treatments initially rendered higher pH than non-treated scaffolds might be associated with partial dissolution of their HCA layers and concomitant ion leaching upon placement into media.

Altogether, media alkalinization, bioactive glass ionic dissolution products and cell morphological features, could have translated into enhanced osteoblastic maturation as shown by increased ALP activity, total protein production, and slightly higher calcium deposition in SBF-treated samples. Further studies could include other bone specific markers, such as osteocalcin protein production, to confirm these findings.

In vivo bone regeneration potential of porous bioactive glass scaffolds in a non-critical size cortical bone defect

Histomorphometric analysis of defects generated in the calvarial bone of rabbits revealed that significantly more bone had formed during a 4 week period of healing in defects treated with 1xSBF pre-treated bioactive glass scaffolds (24.22±1.88 %) compared to non-treated porous bioactive glass scaffolds (15.06±5.75 %), commercially available Bioglass® 45S5 granules (Perioglass®) (12.88±2.13 %), and empty non-treated defects (15.39±1.42 %) (Fig. 9.a, c). Another parameter important for the stable integration of the implant material in bone and indicative for the biocompatibility of the implant material is the bone to implant contact. Carbonated hydroxyapatite (HCA) pre-coated scaffolds induced significantly more bone deposition in direct contact to the implant when compared to the non

carbonated samples (Fig. 9b). Thus, SBF-pre-treatment enhances bone formation in direct contact to the implant. This is also detectable in the histologies (Fig.9d) where glass fibres are being enclosed in the newly formed bone and ongoing bone formation, indicated by the presence of osteoblasts and osteoid, occurring in close proximity to the material.

In terms of mechanical properties, both control defects and Perioglass® are bound to have very low tensile and compression strength at this stage. This is mainly due to the lack of bone repair within the middle of the defect, and in the Perioglass® case, also due to the granular nature of the biomaterial and the lack of interconnectivity. On the other hand, both bioactive glass scaffolds induced bone formation and direct apposition onto the scaffold's fibres, which together with their three dimensional structure of the material may provide better mechanical support within the surrounding tissues. Bone repair and osseointegration were enhanced by SBF treatment (Fig. 9), which can ultimately translate into better mechanical properties, higher tensile strengths matching closer those of native bone and avoidance of stress shielding. The defect model used in this study corresponds to a cortical bone defect, with an elastic modulus of approximately 130 MPa. However, bioactive glass structure and the type of induced bone regeneration in this case is more similar to cancellous bone, which modulus is on average of 50 MPa. [2]

In previous studies, similar scaffolds with porosities between 45-60% were implanted in a pilot study into rabbit tibiae. The results obtained showed their degradation over 6 months, as well as their osteoconductive properties and potential as bone substitute materials.[12] Scaffold's higher porosities were chosen in this work in order to resemble more closely cancellous bone mechanical properties and architecture, as well as to allow for better vascularization.[14]

This initial *in vivo* assessment of porous bioactive glass scaffolds after 1 month revealed better performance when they were pretreated with 1x SBF, although it has yet to be elucidated whether these positive results translate into better bone healing in the longer term.

Other authors have also reported increased bone formation with HCA-precoated bioactive glass, suggesting that the better *in vivo* performance might be caused by the increased protein and growth factor adsorption onto the HCA surface layer, which stimulate in turn osteoblastic adhesion and activity.[21,34,35] Additionally, a higher pH and ionic release might occur in these cases, improving osteoproductive properties, as already mentioned in the previous sections. Overall, both the ionic dissolution of porous scaffolds and the rough surface characteristics of the SBF-treated scaffolds might have translated into enhanced bone regeneration, promoting osteoblastic adhesion, activity, and better bone bonding to them.

To further improve the scaffolds' biological activity, osteoinductive proteins (such as BMP-2) can be co-precipitated within the HCA layer during SBF treatment. This approach could the be applied to promote bone healing in critical size defects and extend the use of these materials.[36]

CONCLUSIONS

The potential of porous bioactive glass scaffolds to promote cell adhesion and activity *in vitro*, as well as bone formation *in vivo* was confirmed in this work, and shown to be enhanced by the presence of a carbonated apatite (HCA) layer on their surface after SBF treatment. This allows for new approaches since the material's inherent osteoconductive and osteopromotive properties are further enhanced, confirming its prospective use in bone regeneration applications.

The authors would like to thank Inion OY (Tampere, Finland) for the supply of the different porous bioactive glass scaffolds and a partial funding of this research. Anne Greet Bitterman (EMZ, University of Zurich) and Paul Hug (EMPA, Dubendorf) for their assistance with SEM and Raman analysis respectively, as well as Alexander Tchouboukov for the histological preparations.

References

1. Acarturk TO, Hollinger JO. Commercially available demineralized bone matrix compositions to regenerate calvarial critical-sized bone defects. Plastic and reconstructive surgery 2006;118:862-873.
2. Hollinger JO, Einhorn TA, Doll, BA, Sfeir, C. Bone tissue engineering. CRC Press, Boca Raton Florida (USA) 2004.
3. Parikh SN. Bone graft substitutes: past, present, future. J Postgrad Med 2002;48:142-148.
4. Hench LL. The story of Bioglass((R)). Journal of materials science 2006;17:967-978.
5. Hench LL, Polak JM. Third generation biomedical materials. Science 2002;295(5557):1014-1017.
6. Hench LL, Paschall HA. Direct chemical bond of bioactive glass-ceramic materials to bone and muscle. J Biomed Mater Res 1973;7:25-42.
7. Hench LL, Wilson J. Surface-active biomaterials. Science 1984;226:630-636.
8. Kokubo T, Takadama H. How useful is SBF in predicting in vivo bone bioactivity? Biomaterials 2006;27:2907-2915.
9. Silver IA, Deas J, Erecinska M. Interactions of bioactive glasses with osteoblasts in vitro: effects of 45S5 Bioglass, and 58S and 77S bioactive glasses on metabolism, intracellular ion concentrations and cell viability. Biomaterials 2001;22:175-185.
10. Oonishi H, et al. Particulate bioglass compared with hydroxyapatite as a bone graft substitute. Clin Orthop Relat Res 1997;334:316-325.
11. Schepers EJ, Ducheyne P. Bioactive glass particles of narrow size range for the treatment of oral bone defects: a 1-24 month experiment with several materials and particle sizes and size ranges. J Oral Rehabil 1997;24:171-181.
12. Moimas L, Biasotto M, Di Lenarda R, Olivo A, Schmid C. Rabbit pilot study on the resorbability of three-dimensional bioactive glass fibre scaffolds. Acta Biomater 2006;2:191-199.
13. Brink M. The influence of alkali and alkaline earths on the working range for bioactive glasses. J Biomed Mater Res 1997;36:109-117.
14. Pirhonen E, Moimas L, Brink M. Mechanical properties of bioactive glass 9-93 fibres. Acta Biomater 2006;2:103-107.
15. *Scofield JH. Hartree-Slater subshell photoionization cross-sections at 1254 and 1487 ev. Journal of Electron Spectroscopy and Related Phenomena 1976;8:129-137.*
16. *Maeda T, Matsunuma, A., Kurahashi, I., Yanagawa, T., Yoshida, H., Horiuchi, N Induction of osteoblast differentiation indices by statins in MC3T3-E1cells. J Cell Biochem 2004;92:458-471.*
17. Revell PA. Histomorphometry of bone. Journal of clinical pathology 1983;36:1323-1331.
18. El-Ghannam A, Ducheyne P, Shapiro IM. Porous bioactive glass and hydroxyapatite ceramic affect bone cell function in vitro along different time lines. J Biomed Mater Res 1997;36:167-180.
19. Penel G, Leroy G, Rey C, Bres E. MicroRaman spectral study of the PO4 and CO3 vibrational modes in synthetic and biological apatites. Calcif Tissue Int 1998;63:475-481.
20. Gonzalez P, Serra J, Liste S, Chiussi S, Leon B, Perez-Amor M. Raman spectroscopic study of bioactive silica based glasses. Journal of non-crystalline solids 2003;320:92-99.
21. *El-Ghannam A, Amin H, Nasr T, Shama A. Enhancement of bone regeneration and graft material resorption using surface-modified bioactive glass in cortical and human maxillary cystic bone defects. Int J Oral Maxillofac Implants 2004;19:184-191.*
22. *Clupper DC, Gough, J. E., Embanga, P. M., Notingher, I., Hench, L. L., Hall, M. M. Bioactive evaluation of 45S5 bioactive glass fibres and preliminary study of human osteoblast attachment. Journal of materials science 2004;15:803-808.*
23. *Massaro C, Baker, M. A. Cosentino, F., Ramires, P. A., Klose, S., Milella, E* Surface and biological evaluation of hydroxyapatite-based coatings on titanium deposited by different techniques. J Biomed Mater Res 2001;58:651-657.
24. Gu YW, Tay BY, Lim CS, Yong MS. Biomimetic deposition of apatite coating on surface-modified NiTi alloy. Biomaterials 2005;26:6916-6923.
25. *Vallet-Regi M, Romero AM, Ragel CV, LeGeros RZ. XRD, SEM-EDS, and FTIR studies of in vitro growth of an apatite-like layer on sol-gel glasses. J Biomed Mater Res 1999;44:416-421.*

26. *Anselme K, Bigerelle, M., Noel, B., Dufresne, E., Judas, D., Iost, A., Hardouin, P. Qualitative and quantitative study of human osteoblast adhesion on materials with various surface roughnesses. J Biomed Mater Res 2000;49:155-166.*
27. *Zhao G, Zinger, O., Schwartz, Z., Wieland, M., Landolt, D., Boyan, B. D.* Osteoblast-like cells are sensitive to submicron-scale surface structure. Clin Oral Implants Res 2006;17:258-264.
28. Gough JE, Notingher I, Hench LL. Osteoblast attachment and mineralized nodule formation on rough and smooth 45S5 bioactive glass monoliths. J Biomed Mater Res A 2004;68:640-650.
29. *Shu R, McMullen R, Baumann MJ, McCabe LR. Hydroxyapatite accelerates differentiation and suppresses growth of MC3T3-E1 osteoblasts. J Biomed Mater Res 2003;67(A):1196-1204.*
30. *Martin JY, Schwartz, Z., Hummert, T. W., Schraub, D. M., Simpson, J., Lankford, J., Jr., Dean, D. D., Cochran, D. L., Boyan, B. D.* Effect of titanium surface roughness on proliferation, differentiation, and protein synthesis of human osteoblast-like cells (MG63). J Biomed Mater Res 1995;29:389-401.
31. Kaysinger KK, Ramp WK. Extracellular pH modulates the activity of cultured human osteoblasts. J Cell Biochem 68, 83-89 (1998).
32. Gough JE, Jones JR, Hench LL. Nodule formation and mineralisation of human primary osteoblasts cultured on a porous bioactive glass scaffold. Biomaterials 2004;25:2039-2046.
33. Xynos ID, Edgar AJ, Buttery LD, Hench LL, Polak JM. Ionic products of bioactive glass dissolution increase proliferation of human osteoblasts and induce insulin-like growth factor II mRNA expression and protein synthesis. Biochem Biophys Res Commun 2000;276:461-465.
34. Kokubo T, Kim HM, Kawashita M. Novel bioactive materials with different mechanical properties. Biomaterials 2003;24:2161-2175.
35. Fujibayashi S, Neo M, Kim HM, Kokubo T, Nakamura TA. Comparative study between in vivo bone ingrowth and in vitro apatite formation on Na2O-CaO-SiO2 glasses. Biomaterials 2003;24:1349-1356.
36. Liu Y, Huse RO, de Groot K, Buser D, Hunziker EB. Delivery mode and efficacy of BMP-2 in association with implants. J Dent Res 2007;86:84-89.

Figure legends

Figure 1. SEM images of (a) scaffold as manufactured (0 SBF) and (b) 1x SBF and 2x SBF pre-treated scaffolds at different magnifications as indicated. Images were obtained from two independent experiments, of at least 3 samples each.

Figure 2. Nodule (including spheres and hemispheres) and cluster count after the two SBF treatments performed. Values shown are means ±SD of two independent experiments, n=4.

Figure 3. Raman spectra performed after the different treatments in simulated body (SBF). Note the peaks at 440, 600, 950 cm^{-1}, typical for HCA formation. Results include two independent experiments, n=3 each.

Figure 4. XPS survey spectra of the different scaffold surfaces.

Figure 5. SEM images of MC3T3-E1 cells on untreated (a-c), 1x SBF (d-f) and 2x SBF-treated scaffolds (g-i) respectively, after 24h in culture.

Figure 6. SEM images of MC3T3-E1 cells after 1 and 4 weeks cultured on 1x SBF and 2x SBF treated scaffolds, respectively. b) Detail of cells cultured on 2x SBF-treated scaffolds after 1 week.

Figure 7. Biological response of MC3T3-E1 cells cultured on BG1 scaffolds. a) ALP activity after 1 week in culture. b) Calcium nodule deposition after 2 weeks. c) Total protein production and d) DNA content after 1 week. Values shown are means ±SD of three independent experiments carried out in triplicate. (*P<0.05, compared to 0 SBF outcome).

Figure 8. Time course of pH values in cell culture supernatants of BG1 scaffolds. Media was exchanged at each of the time points shown. Results shown are means ±SD of two independent experiments.

Figure 9. *In vivo* bone regeneration with different bioactive glass compositions evaluated in a rabbit calvarial defect model. Bone healing in non-critical size defects was assessed 4 weeks after the operation. a) Histomorphometric quantitative analysis of bone formation in the middle section of the defect. Results shown are mean values ±SD, of each condition (n≥3). b) Histomorphometric quantitative analysis of bone to implant contact. Results shown are mean values ±SD, of each condition (n≥3). c) Histological Goldner-Trichrome stained middle sections. The representative examples are from empty control, Perioglass, porous bioactive glass scaffold of 80% porosity, and respective porous-HCA bioactive glass scaffolds. Bone appears dark green, osteoid red and fibrous tissue light green). Scale bar = 1mm. d) Detail of representative porous-HCA bioactive glass scaffold osteoconductive properties (middle of the defect area in Fig. 9.c), (*P< 0.05).

TABLES

TABLE I. Molar composition of blood plasma and SBF.

TABLE II. Surface elemental composition (atomic %) and atomic ratios Ca/P and Ca/O of BG1 scaffolds as manufactured (0 SBF), after SBF treatment (1x SBF, 2x SBF), and theoretical Hydroxyapatite (HAP) values.

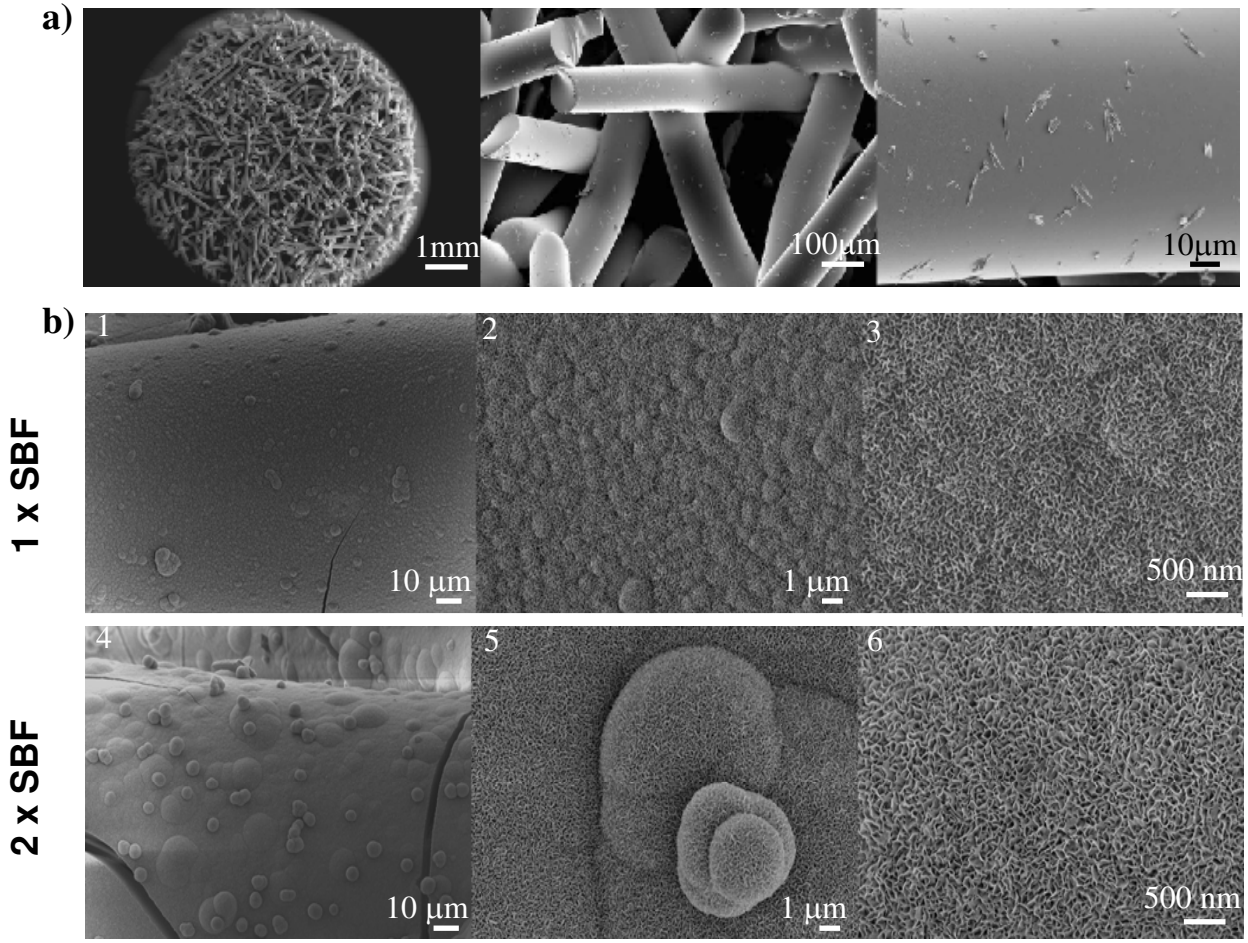
a)
1mm
100µm
10µm
b)
1 x SBF
2 x SBF
1
2
3
10 µm
1 µm
500 nm
4
5
6
10 µm
1 µm
500 nm

Fig 1

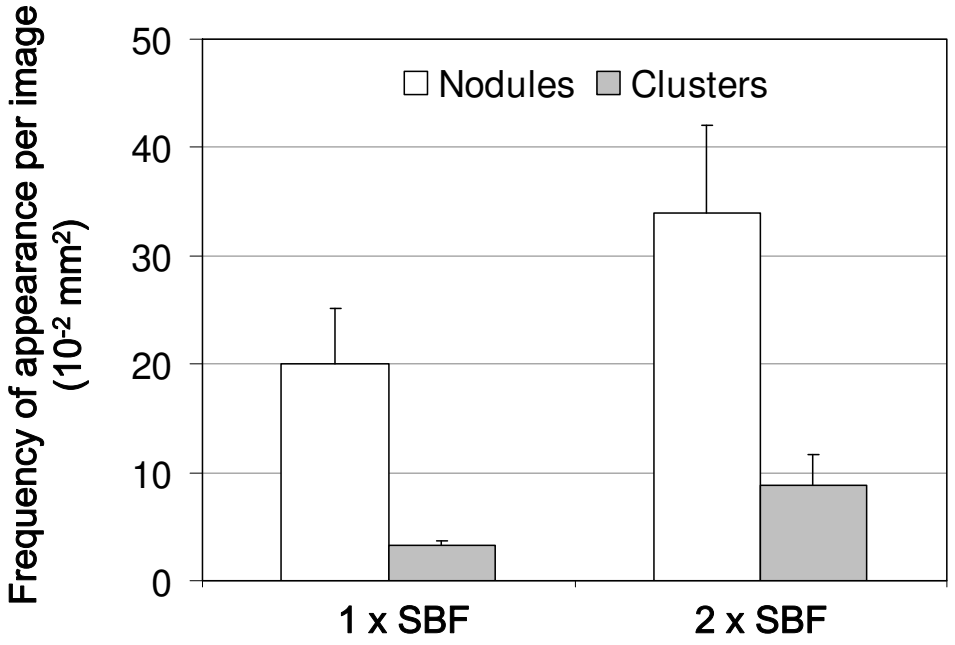
Frequency of appearance per image
(10-2 mm2)
50
40
30
20
10
0
Nodules
Clusters
1 x SBF
2 x SBF

Fig 2

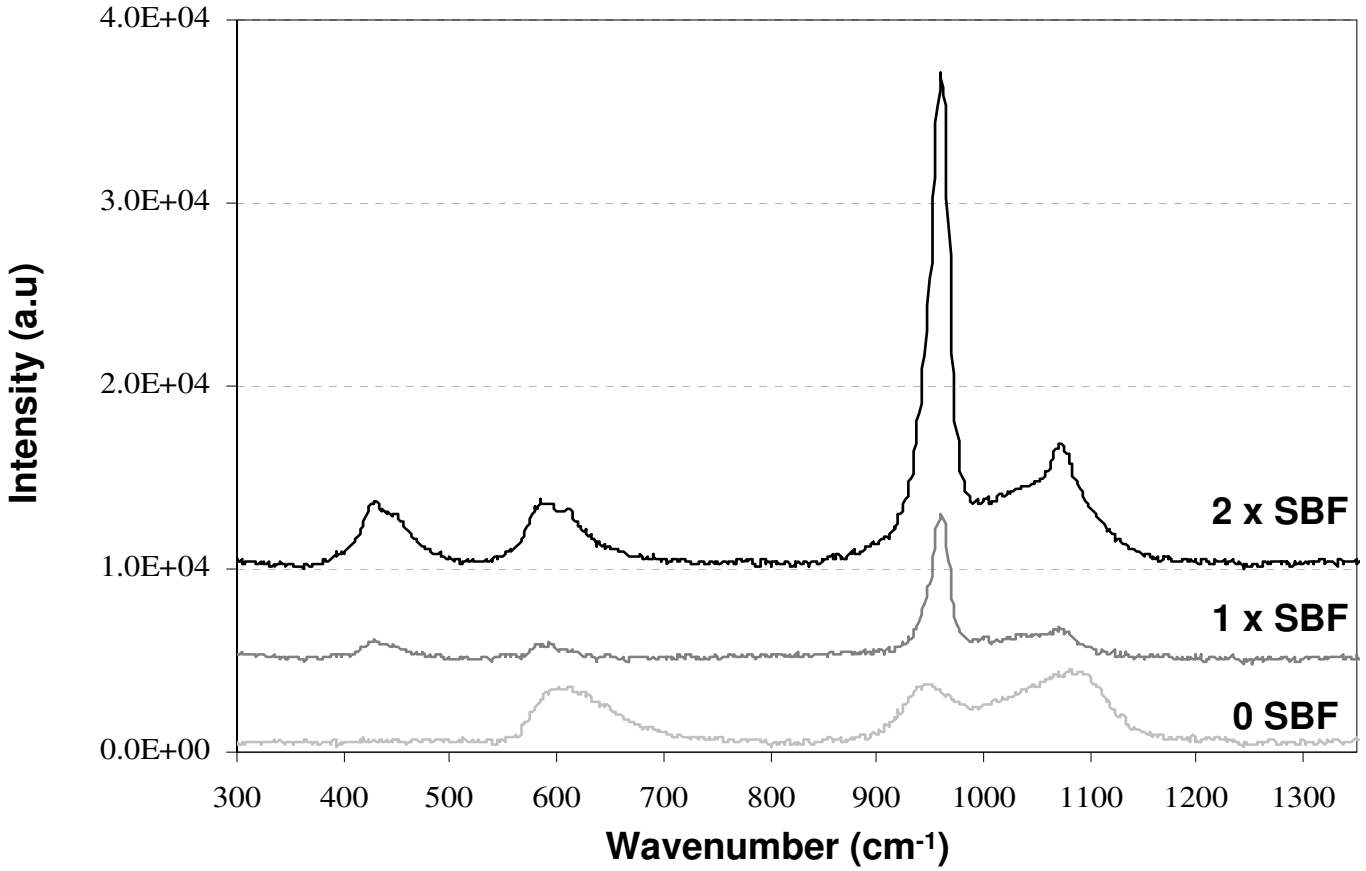
4.0E+04
3.0E+04
2.0E+04
1.0E+04
0.0E+00
Intensity (a.u)
2 x SBF
1 x SBF
0 SBF
300
400
500
600
700
800
900
1000
1100
1200
1300
Wavenumber (cm-1)

Fig 3

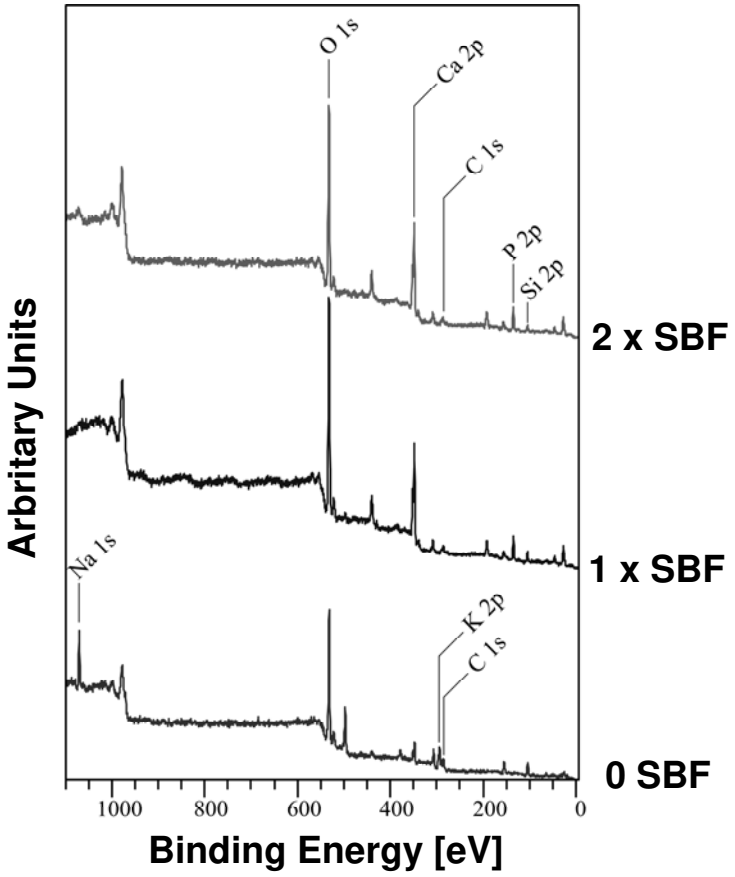
O 1s
Ca 2p
C 1s
P 2p
Si 2p
2 x SBF
1 x SBF
Na 1s
K 2p
C 1s
0 SBF
Arbritary Units
1000
800
600
400
200
0
Binding Energy [eV]

Fig 4

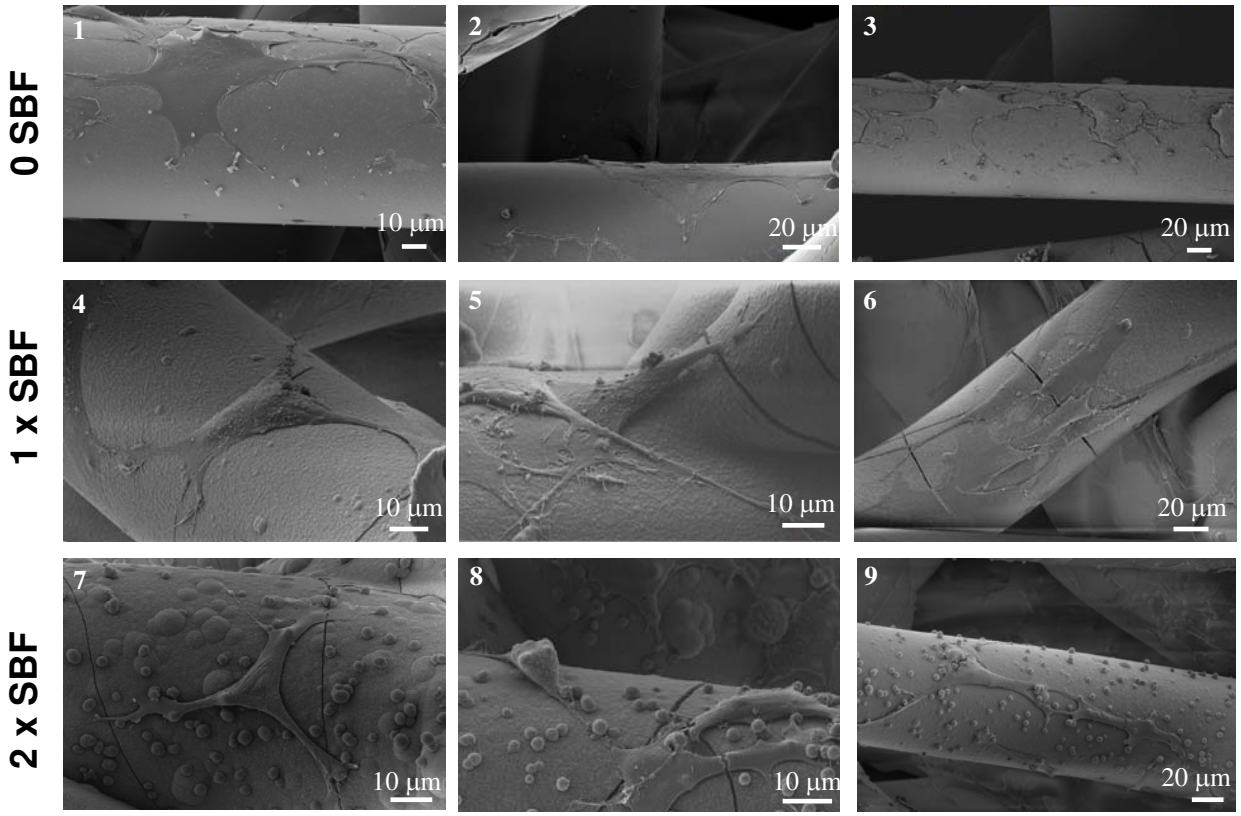
0 SBF
1 x SBF
2 x SBF
1
2
3
4
5
6
7
8
9
10 µm
20 µm
10 µm
20 µm
10 µm
10 µm
20 µm
10 µm
10 µm
20 µm

Fig 5

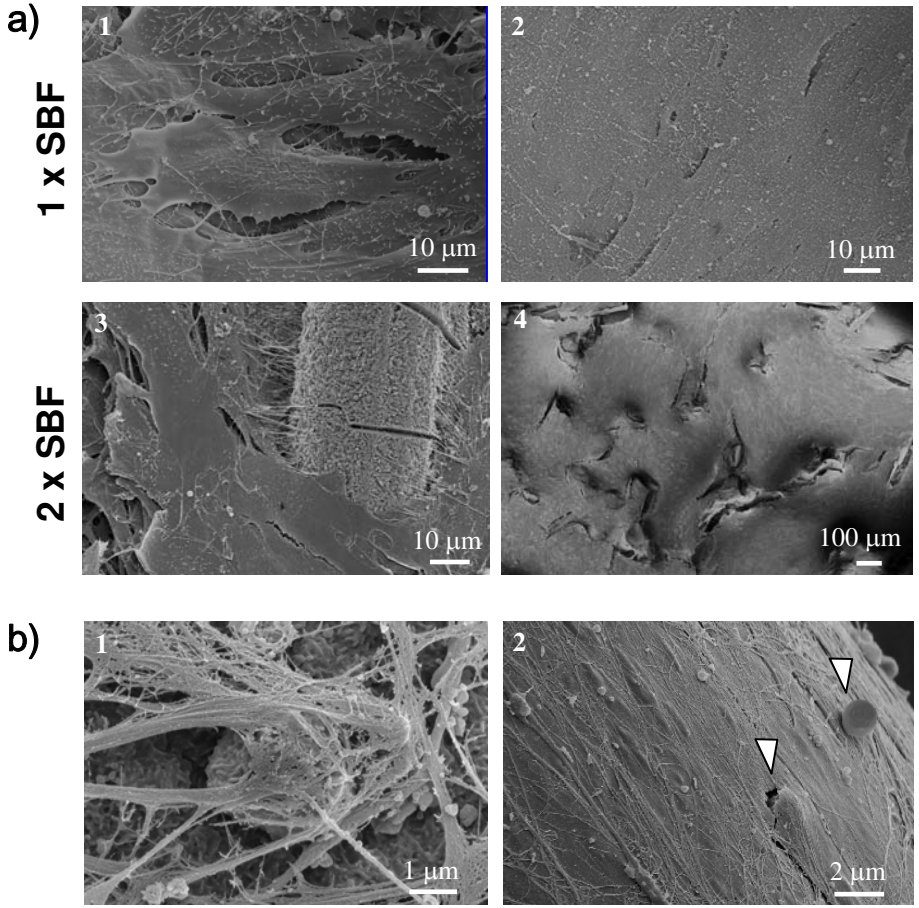

Fig 6

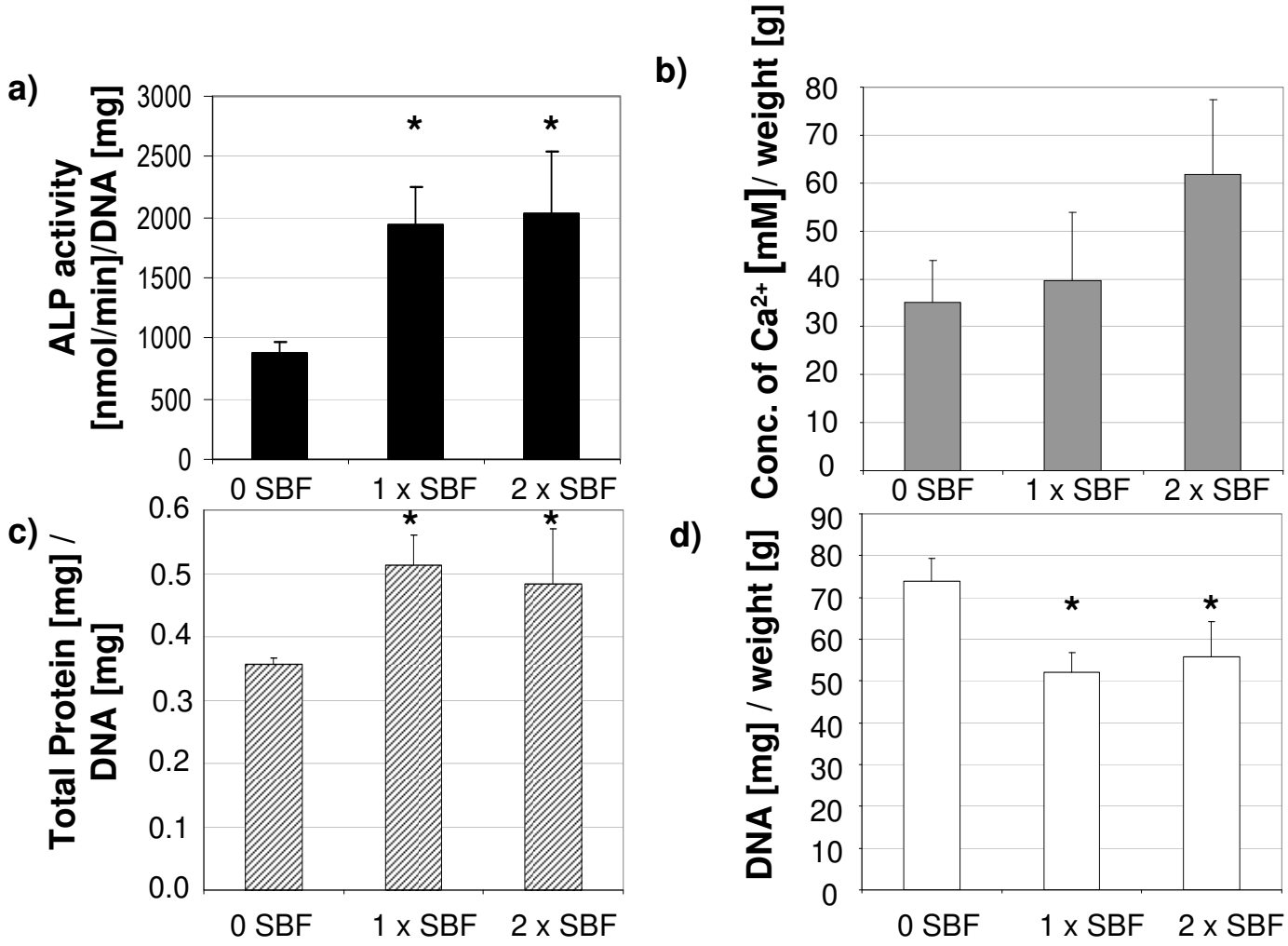
a)
ALP activity [nmol/min]/DNA [mg]
3000
2500
2000
1500
1000
500
0
*
*
0 SBF
1 x SBF
2 x SBF
b)
Conc. of Ca2+ [mM]/ weight [g]
80
70
60
50
40
30
20
10
0
0 SBF
1 x SBF
2 x SBF
c)
Total Protein [mg] / DNA [mg]
0.6
0.5
0.4
0.3
0.2
0.1
0.0
*
*
0 SBF
1 x SBF
2 x SBF
d)
DNA [mg] / weight [g]
90
80
70
60
50
40
30
20
10
0
*
*
0 SBF
1 x SBF
2 x SBF

Fig 7

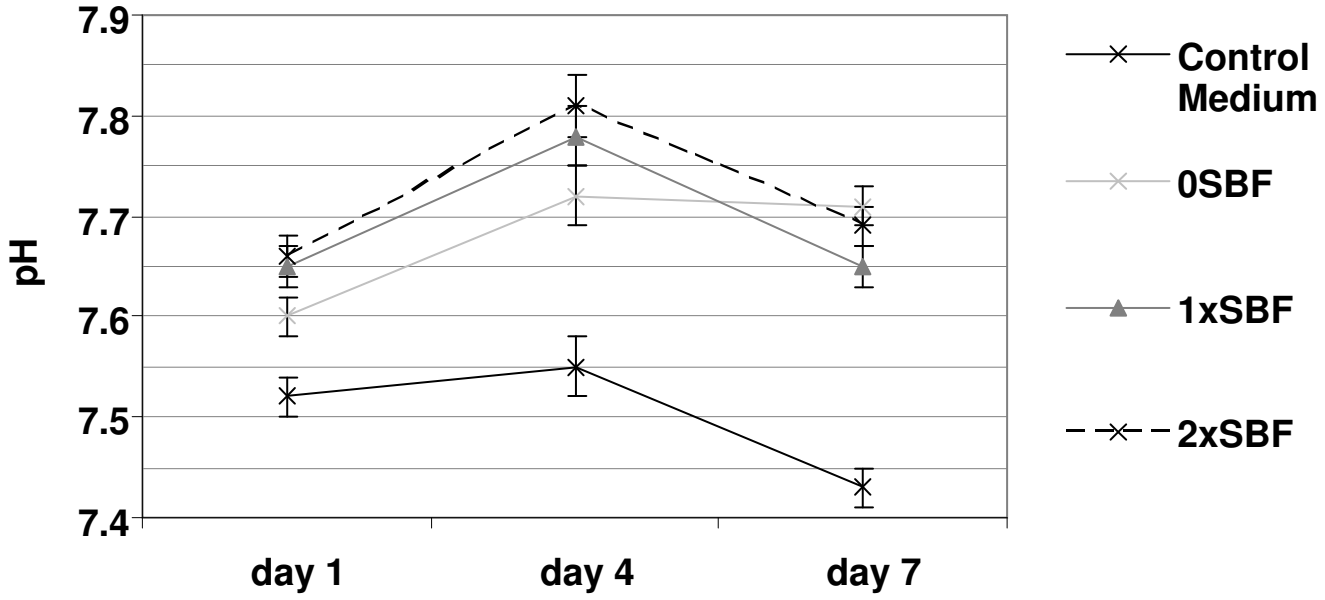
7.9
7.8
7.7
7.6
7.5
7.4
pH
day 1
day 4
day 7
Control Medium
0SBF
1xSBF
2xSBF

Fig 8

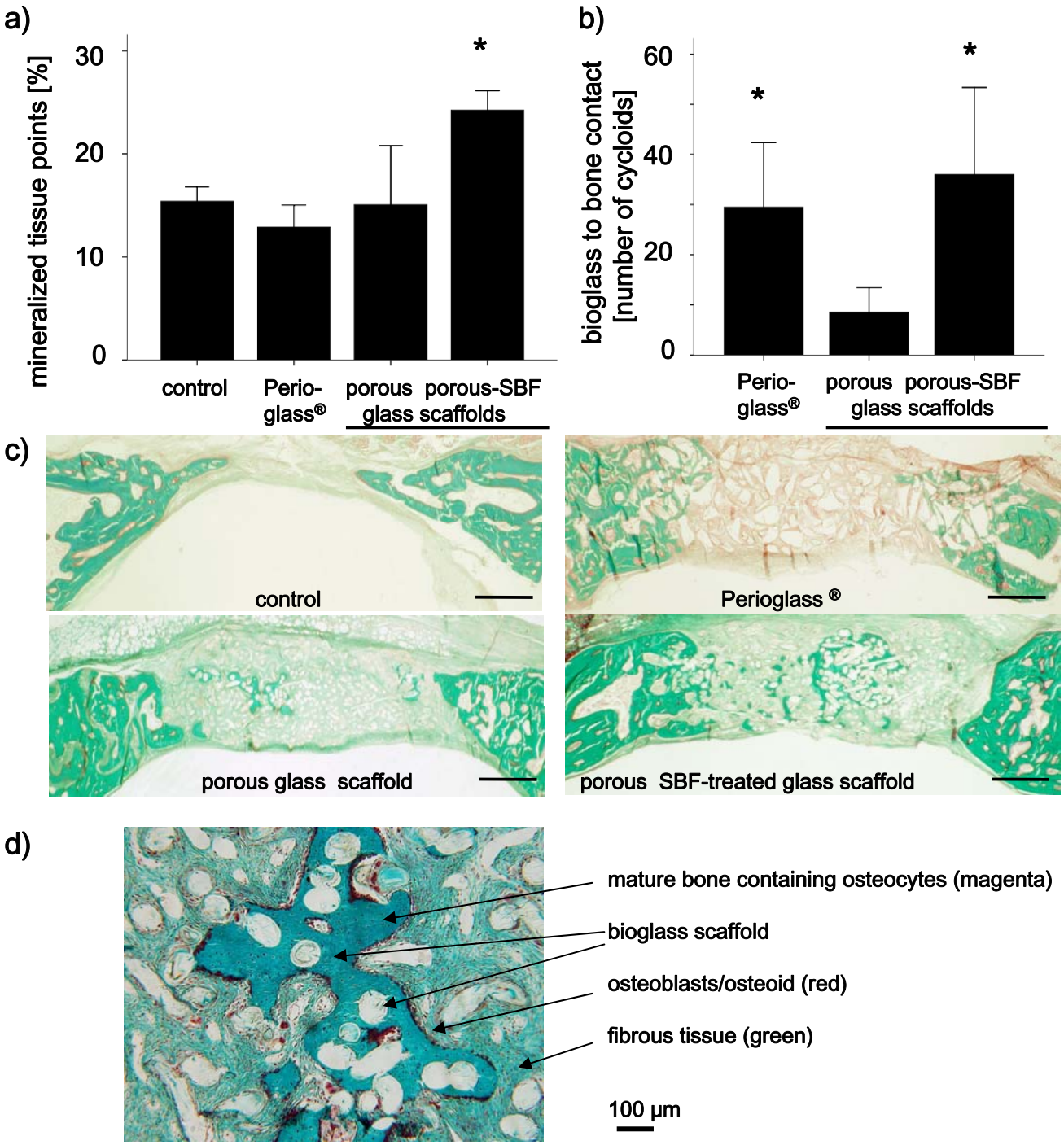
a)
mineralized tissue points [%]
30
20
10
0
*
control
Perio-glass®
porous glass scaffolds
porous-SBF
b)
bioglass to bone contact [number of cycloids]
60
40
20
0
*
*
Perio-glass®
porous glass scaffolds
porous-SBF
c)
control
Perioglass ®
porous glass scaffold
porous SBF-treated glass scaffold
d)
mature bone containing osteocytes (magenta)
bioglass scaffold
osteoblasts/osteoid (red)
fibrous tissue (green)
100 µm

Fig 9